Chapter 7
Combustion Process and Air Emission Formation

The combustion thermochemistry introduced in Chap. 3 applies to only simple cases. In engineering practice, fuels and oxidizers are seldom premixed to avoid explosion. Instead, they are often delivered separately into the combustion chamber and then mixed immediately prior to combustion. The combustion takes place in a flame rather than the entire combustion system. As a result, the physical processes as well as the fuel properties govern actual fuel combustion. Fluid mechanics, thermodynamics, and heat and mass transfer govern the fuel-oxidizer mixing, the combustion process, and air emissions.

In the process of combustion, the chemical energy of fuel is converted into thermal energy. There are a variety of fuels used in combustion for energy production in different engineering applications. The fuels can be solid, liquid, gaseous, or their mixtures. Each of them also has its own family. Most commonly used solid fuels include coal, charcoal, coke, and biomass; liquid ones include gasoline, diesel, and recently, bioethanol and biodiesel. Natural gas is the most widely used gaseous fuel which contains primarily methane (CH_4) and other trace gases.

Depending on the fuel properties the flue gases may contain high concentrations of the oxides of sulphur and nitrogen (SO_x, and NO_x), fine particulates, and trace elements like mercury. The actual combustion processes and their air emission formation mechanisms are introduced in this chapter.

7.1 Gaseous Fuel Flame

Gaseous fuels and oxidizers enter a stationary combustion device separately and combustion takes place in a diffusion flame (Fig. 7.1). The combustion sustains by the heat released from combustion. Mixing ratio is described using the overall equivalence ratio introduced in Sect. 3.2. However, this value is not uniform everywhere and the local equivalence ration varies from 0 to 1, representing zones of pure oxidizer or pure fuel. When the gaseous fuel is injected into the combustion chamber, there is a central core area containing pure fuel. The surrounding oxidizer and outer

Z. Tan, *Air Pollution and Greenhouse Gases*, Green Energy and Technology,
DOI 10.1007/978-981-287-212-8_7

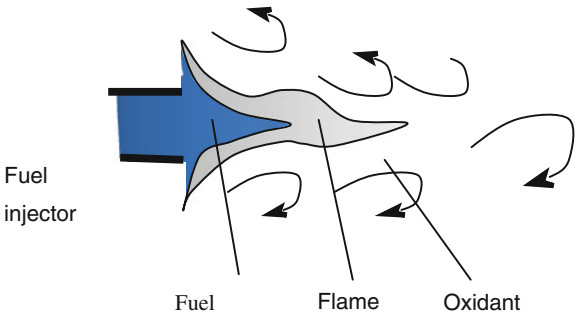

Fig. 7.1 Schematic diagram of conventional diffusion flame

part of the fuel core are mixed by diffusion forming a layer that enables combustion at an equivalence ratio of around 1, which defines the diffusion flame. Main combustion occurs in this diffusion flame. At the location that is closer to the injector, fuel rich combustion takes place resulting in soot particle formation.

Turbulent mixing is required to achieve high combustion efficiency and low air emissions of soot, CO, HC, and so on. As a result, more energy is needed to inject the fuel gas at the same flow rate. This energy consumption increases as the fifth power of the burner size [13]. Multiple small burners rather than a single large one can be employed in large facility.

7.2 Liquid Fuel Combustion

Liquid fuels are atomized and burned in the form of droplets. They can be burned in both stationary (such as a power plant) and mobile systems (like a truck engine). The combustion efficiency and the air emissions depend on the fuel type as well as the size and volatility of the fuel droplets.

The particle dynamics introduced in Chap. 4 can be used to describe the droplet dynamics in the combustion chamber. It has been found that the droplet drag coefficient is very close to that for a solid sphere of the same diameter [49], therefore, it is reasonable to assume that fine spray droplets would follow the carrier gas in a combustion chamber and the motion is in the Stokes region, i.e., $Re_p < 1$ (see Sect. 4.1.2). The corresponding drag coefficient is then described as

$$C_D = 24/Re_p \tag{7.1}$$

At high Reynolds number, large droplets may break into smaller ones and these small droplets will have low Reynolds numbers again. In many practical combustion analyses, we can assume laminar flow near the droplet surface.

When the fuel droplets enter a combustion system, elevated surrounding temperature enables the evaporation of the droplets and combustion takes place between the oxidizer and the fuel vapors.

7.2.1 Droplet Vaporization

There have been many models for fuel droplet evaporation in spray combustion. Most of them describe fuel droplets as spherical; the only relative motion between the droplets and gas involves radial convection due to vaporization. A critical review was given by Sirignano [42] for droplet vaporization in a high-temperature environment. However, it would deviate too much from the scope of this book if we continued on the combustion theories. For this reason, only a simple analysis is introduced as follows.

The energy required to vaporize a fuel droplet can be calculated using

$$q' = c_{\mathrm{p}}(T_{\mathrm{v}} - T_0) + h_{\mathrm{fg}} \tag{7.2}$$

where c_{p} is the specific heat of the fuel, T_{v} is the vaporization temperature for the liquid fuel (K), T_0 is the initial temperature when the droplets are sprayed into the combustion system, and h_{fg} is the latent heat of vaporization of the fuel (J/mol). The energy needed for the vaporization of the liquid droplets is taken from the surrounding gases by thermal radiative and conductive heat transfer, which can be found in many advanced heat and mass transfer books.

The droplet size decreases as the evaporation proceeds. Assuming vapor velocity profile is symmetric around the center of the droplet and the rate of vaporization is described as

$$\dot{m}_{\mathrm{v}} = \rho_{\mathrm{v}} u 4\pi r^2 = \rho_{\mathrm{v}} u_{\mathrm{s}} 4\pi r_{\mathrm{s}}^2 \tag{7.3}$$

where $\dot{m}_{\mathrm{v}}$ is the vaporization rate (kg/s); it is also the loss rate with respective to the liquid droplet. ρ_{v} is vapor density, u_{s} is the vapor speed leaving the surface and r_{s} is the radius of the droplet. $4\pi r_{\mathrm{s}}^2$ is the surface area of the droplet sphere.

Assuming that only conductive heat transfer dominates and that the radial profiles of temperature and compositions are quasi-steady, the change of the droplet diameter can be related to the heat transfer from the surrounding to the droplet surface. Conservation of energy for the droplet leads to

$$\dot{m}_{\mathrm{v}} c_{\mathrm{p}}(T - T_{\mathrm{v}}) + \dot{m}_{\mathrm{v}} h_{\mathrm{fg}} = 4\pi r^2 k \frac{\mathrm{d}T}{\mathrm{d}r} \tag{7.4}$$

where T is the temperature at r, k is the thermal conductivity of the liquid droplet at the surface. LHS is the energy for liquid evaporation and RHS is for the heat transfer by conduction.

The fuel vapor resulted from the evaporation is then transported by diffusion and convention from the surface of the droplet to the surrounding gas phase. The corresponding convective diffusion can be described as

$$\dot{m}_{\mathrm{v}}(1-f_{\mathrm{v}}) = -4\pi r^2 \rho_{\mathrm{v}} D \frac{\mathrm{d}f_{\mathrm{v}}}{\mathrm{d}r} \tag{7.5}$$

where f_{v} is the vapor mass fraction at the droplet surface. D is the diffusivity of the vapor in the surrounding gas phase.

Integration of Eqs. (7.4) and (7.5), respectively, from the droplet surface $r = r_{\mathrm{s}}$ to $r \to \infty$ leads to

$$\ln\left(\frac{T_{\mathrm{s}} - T_{\mathrm{v}} + h_{\mathrm{fg}}/c_{\mathrm{p}}}{T_{\infty} - T_{\mathrm{v}} + h_{\mathrm{fg}}/c_{p}}\right) = -\left(\frac{c_{\mathrm{p}}}{4\pi k}\right)\frac{\dot{m}_{\mathrm{v}}}{r_{\mathrm{s}}} \tag{7.6}$$

$$\ln\left(\frac{1-f_{\mathrm{v,s}}}{1-f_{\mathrm{v},\infty}}\right) = -\left(\frac{1}{4\pi\rho_{\mathrm{v}} D}\right)\frac{\dot{m}_{\mathrm{v}}}{r_{\mathrm{s}}} \tag{7.7}$$

where subscript s is the for the droplet surface. T_{s} is the surface temperature of the droplet. Equation (7.6) gives the evaporation rate as

$$\dot{m}_{\mathrm{v}} = \frac{4\pi r_{\mathrm{s}} k}{c_{\mathrm{p}}} \times \ln\left[\frac{c_{\mathrm{p}}(T_{\infty} - T_{\mathrm{v}}) + h_{\mathrm{fg}}}{c_{\mathrm{p}}(T_{\mathrm{s}} - T_{\mathrm{v}}) + h_{\mathrm{fg}}}\right]. \tag{7.8}$$

At thermodynamic equilibrium state, the surface temperature is assumed to be the same as the vaporization temperature, $T_{\mathrm{s}} \approx T_{\mathrm{v}}$, then Eq. (7.8) is simplified as

$$\dot{m}_{\mathrm{v}} = \frac{4\pi r_{\mathrm{s}} k}{c_{\mathrm{p}}} \ln\left[1 + \frac{c_{\mathrm{p}}(T_{\infty} - T_{\mathrm{s}})}{h_{\mathrm{fg}}}\right]. \tag{7.9}$$

Conservation of mass leads to the relationship between the mass of the droplet $m_{\mathrm{l}} = \rho_{\mathrm{l}}(4\pi/3)r_{\mathrm{s}}^3$ and the vaporation rate can is $\dot{m}_{\mathrm{v}} = -\mathrm{d}m_{\mathrm{l}}/\mathrm{d}t$

$$\dot{m}_{\mathrm{v}} = -\frac{\mathrm{d}m_{\mathrm{l}}}{\mathrm{d}t} = \frac{\mathrm{d}}{\mathrm{d}t}\left(\frac{4}{3}\pi\rho_{\mathrm{l}} r_{\mathrm{s}}^3\right) = -4\pi\rho_{\mathrm{l}} r_{\mathrm{s}}^2 \frac{\mathrm{d}r_{\mathrm{s}}}{\mathrm{d}t}. \tag{7.10}$$

Combination of Eqs. (7.9) and (7.10) leads to

$$-4\pi\rho_{\mathrm{l}} r_{\mathrm{s}}^2 \frac{\mathrm{d}r_{\mathrm{s}}}{\mathrm{d}t} = \frac{4\pi r_{\mathrm{s}} k}{c_{\mathrm{p}}} \times \ln\left[1 + \frac{c_{\mathrm{p}}(T_{\infty} - T_{\mathrm{s}})}{h_{\mathrm{fg}}}\right]$$

$$-r_{\mathrm{s}}\,\mathrm{d}r_{\mathrm{s}} = \left\{\frac{k}{\rho_{\mathrm{l}} c_{\mathrm{p}}} \ln\left[1 + \frac{c_{\mathrm{p}}(T_{\infty} - T_{\mathrm{s}})}{h_{\mathrm{fg}}}\right]\right\}\mathrm{d}t. \tag{7.11}$$

As a simplification, the term in { } can be assumed constant at quasi-steady state. Then the droplet diameter over time can be determined by integration from the initial droplet diameter $r_s = r_{s0}$ at $t = 0$ and r_s at any time t.

$$-\int_{r_{s0}}^{r_s} r_s \, dr_s = \int_0^t \left\{ \frac{k}{\rho_l c_p} \ln\left[1 + \frac{c_p(T_\infty - T_s)}{h_{fg}}\right] \right\} dt \tag{7.12}$$

$$\frac{1}{2}\left(r_{s0}^2 - r_s^2\right) = \frac{tk}{\rho_l c_p} \ln\left[1 + \frac{c_p(T_\infty - T_s)}{h_{fg}}\right] \tag{7.13}$$

Equation (7.13) can be used to estimate the time for a liquid fuel droplet to complete vaporization, or life time of the droplet. Substitute $r_s = 0$ into Eq. (7.13), we have

$$t_e = \frac{r_{s0}^2}{\frac{2k}{\rho_l c_p} \cdot \ln\left[1 + \frac{c_p(T_\infty - T_s)}{h_{fg}}\right]} \tag{7.14}$$

The lifetime of the droplets increases with their sizes, and it is in the order of millisecond [42]. The life time t_e is important to characterize the combustion efficiency of atomized liquid fuel droplets and the consequent air emissions. If t_e is longer than the residence time of the combustion system, the droplets will not be burned completely because of incomplete vaporization. As a result, liquid fuel droplets exist in the flue gas (or exhaust). They may be part of the particulate emissions. Meanwhile residual fuel evaporation continues but these extra vapors are not burned at low temperature; this result in extra volatile organic compound (VOC) emissions.

Since t_e is proportional to the square of initial droplet diameter, r_{s0}^2, it is imperative that fine spray droplets favor combustion efficiency and lower the air emissions. However, the upper limit of the droplet size depends on the design of nozzles employed.

7.2.2 Vapor Combustion

When the combustible vapor is mixed with the oxidizers at high temperature, combustion takes place in a thin flame surrounding the droplet. As depicted in Fig. 7.2, vapor concentration decreases from the droplet surface r_s to the flame r_f, and vapor is oxidized instantaneously in the thin flame. Oxidizer is transported to the flame from the surrounding environment by diffusion that is driven by the concentration gradient. Part of the heat produced by the combustion is transferred to the surface of the fuel droplet to sustain the droplet vaporization. Combustion in the zone between the flame and the droplet surface is highly fuel rich due to the great fuel vapor concentration, and the combustion products join the vapor as combustible gases. The combustion at $r > r_f$ is fuel lean and complete owing to the sufficient oxygen supply.

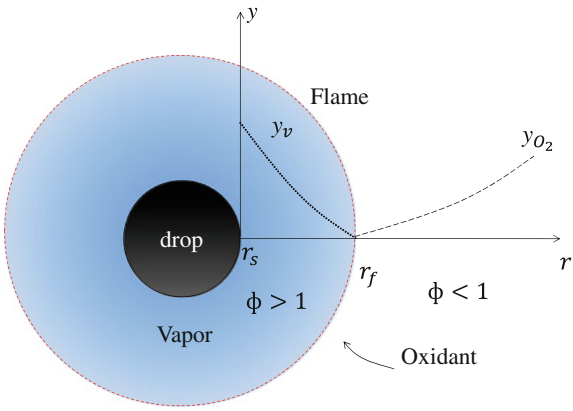

Fig. 7.2 Single droplet combustion model

7.3 Solid Fuel Combustion

7.3.1 Solid Fuels

Solid fuels are easy to transport, store, and produce. They have moderate ignition temperature. They are mainly used for combustion in stationary combustion processes; the combustion products are characterized with high ash content and low combustion efficiency. Coal is the most abundant solid fuel. It represents about 1/3 of the global primary energy production. The top five coal consumers are China, USA, India, Russia, and Germany.

In the combustion stoichiometry analysis (Chap. 3), the chemical formula of the fuel has to be determined. Properties of typical solid fuels are determined by proximate analysis and ultimate analysis.

- Proximate analysis of solid fuels determines moisture, volatile matter, ash, and fixed carbon (in coals and cokes) to rank the fuels by comparing the ratio of combustible to incombustible constituents.
- Ultimate analysis provides more information to include elemental analysis so the simplified chemical formula can be obtained for stoichiometry analysis.

ASTM International Standard [1] (MNL11271M, Proximate Analysis) specifies how to conduct the proximate analysis of coal. The result separates the products into four groups:

(1) moisture,
(2) volatile matter, consisting of gases and vapors driven off during pyrolysis,
(3) fixed carbon, the nonvolatile fraction of coal, and
(4) ash, the inorganic residue remaining after combustion.

Table 7.1 Examples of proximate analysis and ultimate analysis results

Coal rank	Proximate analysis (wt% as received)			
	Fixed carbon	Volatile matter	Moisture	Ash
Anthracite	81.1	7.7	4.5	6.0
Bituminous	54.9	35.6	5.3	4.2
Subbituminous	43.6	34.7	110.5	11.2
Lignite	27.8	24.9	36.9	10.4

Coal Rank	Ultimate Analysis (wt% moisture and ash free)					Net Heating Value (moisture and ash free) (MJ/kg)
	C	H	O	N	S	
Anthracite	91.8	3.6	2.5	1.4	0.7	36.2
Bituminous	82.8	5.1	10.1	1.4	0.6	36.1
Subbituminous	76.4	5.6	14.9	1.7	1.4	31.8
Lignite	71.0	4.3	23.2	1.1	0.4	26.7

Source Higman and van Burgt [27]

Another ASTM International Standard [2] (MNL11272M, Ultimate Analysis) describes how to conduct the ultimate analysis of coal and coke. It determines the carbon, hydrogen, sulfur, nitrogen, and ash in the material as a whole, and estimates the amount of oxygen by difference.

Examples of proximate analysis and ultimate analysis results are shown in Table 7.1.

Example 7.1: Fuel formula In an ultimate analysis of a bituminous coal, elemental analysis shows that the weight fractions of C, H, O, N, and S are, respectively, 82.8, 5.1, 10.1, 1.4, and 0.6. Determine its molecular formula.

Solution From the elemental analysis result, we have Table 7.2. Therefore, the molecular formula can be described as $C_{184}H_{136}O_{16.83}N_{2.67}S$
Note that the sulfur content is 0.6 %, and it is considered as low sulfur coal.

Table 7.2 Fuel formula calculation in Example 7.1

Element	C	H	O	N	S
Fraction (%)	82.8	5.1	10.1	1.4	0.6
Mass/mole	12	1	16	14	16
Mole weight	6.90	5.10	0.63	0.10	0.04
Normalized against S	184	136	16.83	2.67	1

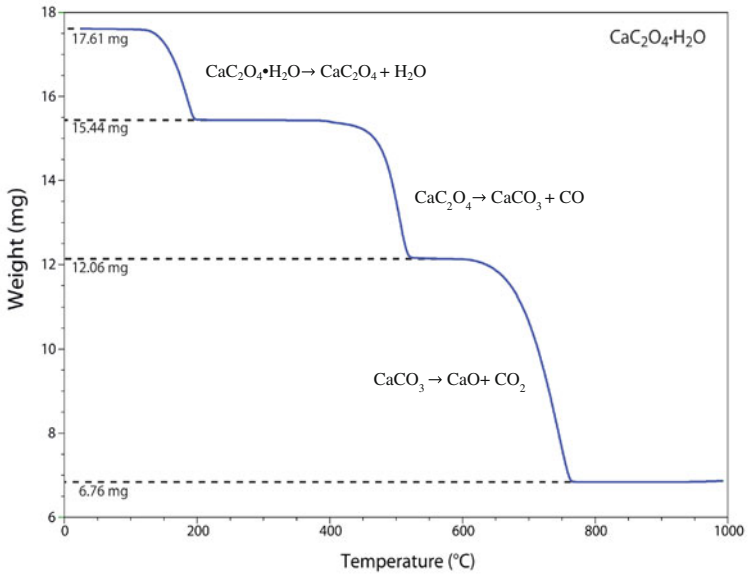

Fig. 7.3 An example of TGA analysis results (used with permission from David Harvey, DePauw University)

- Thermogravimetric analysis
  ASTM specified methods are time-consuming and require a significant amount of samples. An alternative method is thermogravimetric analysis (TGA), which requires a small sample size and gives results fast.

Figure 7.3 shows an example of TGA analysis. It was obtained for $CaC_2O_4 \cdot H_2O$ by heating a sample of 17.61 mg from room temperature to 1,000 °C at a rate of 20 °C/min [23]. Each change in mass results from the loss of a volatile products, and chemical compositions of the volatile products can be determined.

By using the values in Fig. 7.3, we can determine that the resultant gaseous products include, step by step from low to high temperature, 2.17 mg of water, 3.38 mg of carbon monoxide, and 5.30 mg of carbon dioxide. The final residue is CaO.

7.3.1.1 Coal Classification

ASTM (D388–12) Standard, *Classification of Coals by Rank*, defines the rank of coals quantitatively. The rank of a coal is determined based on its degree of metamorphism or alternation (or in a plain word, age). In the order of progressive alternation, coals can be classified into

- Peat
- Lignite coal

- Sub-bituminous coal
- Bituminous coal, and
- Anthracite coal

Peat is considered as the youngest coal in Europe and Asia, but it is considered as biomass in Canada. In Northern Ontario, the Ring of Fires, there is a great amount of peat covered in the forest. The majority of its weight (about 95 %) is water and it requires extensive energy to dry it before combustion, and the consequent thermal efficiency is the lowest.

By underground heating and pressurizing over thousands of years, peat becomes lignite. Lignite is also considered as an immature coal because of its high water content and low heating value. As time passes, lignite becomes darker and harder as sub-bituminous coal followed by bituminous and finally anthracite coals. This terminal rank represents the ultimate maturation of coals.

7.3.2 Solid Fuel Combustion

Solid fuels, coal or biomass, are burned after size reduction. Pulverized coal or biomass can be as small as few micrometers and most of them are smaller than 0.2 mm by mass. They are injected into a furnace where it is mixed with oxidants for combustion.

The combustion process of these solid particles is modeled by

- devolatilization or pyrolysis,
- volatile combustion, and
- char combustion.

7.3.2.1 Devolatilization

Devolatilization or pyrolysis is a complicated process that involves heat and mass transfer as well as chemical decompositions. In general, when a coal particle enters a combustion chamber where the gas is hot, the heating results in the release of volatiles from the pores of the coal particle. The greater the heating rate, the faster the volatiles release. Meanwhile, the size of the particle changes too. Typical heating rate in a pulverized coal combustor is about $10^4 - 10^5$ K/s and the corresponding local temperature may be as high as 2,100 K [14].

The simplest model for this process is a single step model based on a global kinetics that applies to most solid fuels like coal, biomass, and plastic [48].

$$\text{Fuel} \xrightarrow{k_f} xV + (1-x)\text{Ch} \tag{7.15}$$

where V and Ch stand for volatiles and chars, respectively.

Two-step models take into consideration the heating rate and the competition between different volatiles.

$$\begin{aligned} \text{Fuel} &\xrightarrow{k_{f1}} x_1 V_1 + (1 - x_1)\text{Ch}_1 \\ \text{Fuel} &\xrightarrow{k_{f2}} x_2 V_2 + (1 - x_2)\text{Ch}_2 \end{aligned} \tag{7.16}$$

This simplified reaction formula indicates that the particle after devolatilization is decomposed into volatiles and chars, and there is nothing else. The corresponding reaction rate can be described using (modified) Arrhenius expressions

$$k_i = A_i \exp\left(-\frac{E_i}{RT}\right); \quad i = 1, 2 \tag{7.17}$$

With the 2-step model, the conversion rate of the fuel can be described as

$$-\frac{\mathrm{d}x_F}{\mathrm{d}t} = k_{f1} x_F + k_{f2} x_F \tag{7.18}$$

where x_F is the remaining mass fraction of the solid fuel. The 2-Step model parameters are summarized in Table 7.3.

The 1-step model is easy to use but it could not produce a good agreement over a broad temperature range. The 2-step model is more practical for its ease to use and reasonable kinetic agreement over a wide range of temperature; however, it is not based on physical mechanisms [14]. Other models for devolatilization can be found in literature, e.g., the report by Fletcher [14].

Table 7.3 Parameters for calculation of reaction rates of 2-step devolatilization

$k_{f1} = A_1 \exp\left(-\frac{E_1}{RT}\right)$	$k_{f2} = A_2 \exp\left(-\frac{E_2}{RT}\right)$	References
$A_1 = 2.0 \times 10^5$	$A_2 = 1.3 \times 10^7$	[30]
E_1 = 25,000	E_2 = 40,000	
$x_1 = 0.3$	$x_2 = 1.0$	
$A_1 = 3.7 \times 10^5$	$A_2 = 1.46 \times 10^{10}$	[46]
E_1 = 17,600	E_2 = 60,000	
$x_1 = 0.39$	$x_2 = 0.8$	
$A_1 = 3.7 \times 10^5$ (1/s)	$A_2 = 1.46 \times 10^{10}$ (1/s)	[43]
$E_1/R = 8{,}857$ K	$E_2/R = 30{,}200$ K	
x_1 = proximate analysis volatile matter	x_2 = 0.8	

7.4 Formation of VOCs and PAHs

Volatile organic compounds are a family of organic compounds that are volatile in nature. They are mainly lower (C_1–C_4) paraffin, olefins, aldehydes (e.g., formaldehyde), ketones (e.g., acetone) and aromatics (e.g., benzene, toluene, benzaldehyde, phenol). Sometimes, polycyclic aromatic hydrocarbon (PAH) (boiling point 218 °C) is also referred to as a VOC. The organic compounds that are not involved in the formation of smog such as methane, CO, and halogenated organics like 1,1,1-trichloroethane and CFCs are not considered as VOCs.

PAHs are produced during combustion when temperature is about 500–800 °C, and they are oxidized further above 800 °C. Therefore, PAHs mainly present in the low temperature zone of the flame or a combustion facility due to the poor fuel/oxygen mixing. Heavy duty diesel engines (mainly trucks) emit ~1,300 μg/km of lighter PAHs such as pyrene, fluoranthene, etc. while gasoline-fueled cars emit ~100 μg/km of more hazardous heavier PAHs such as benzo(a)pyrene and dibenz(a,h)anthracene [36].

7.5 Formation of CO and CO_2

7.5.1 Volatile Oxidation

The volatiles from liquid fuel vaporization or solid fuel devolatilization contain various combustible gas molecules. It is challenging to decide their exact formula if we were to use the combustion principles introduced in Chap. 3. Alternatively, we can use a simple step reaction model [48] for volatile combustion. Assuming oxygen is the oxidant,

$$\text{Volatiles} + O_2 \xrightarrow{k_{f1}} CO + H_2O \tag{7.19}$$

$$CO + \frac{1}{2}O_2 \xrightarrow{k_{f2}} CO_2. \tag{7.20}$$

The rate of combustion really depends on the rate of mixing.

Another key factor is the heat of combustion of the volatiles, which can be calculated or experimentally determined. With this information known, the reaction rate can be estimated using the combustion kinetics introduced in Chemical Kinetics and Chemical Equilibrium in Chap. 3.

7.5.2 Char Oxidation

Similar to the volatile oxidation analysis above, a simple model [13, p. 150] for the oxidation of char or other similar solid carbon-based fuels is

$$C_s + \frac{1}{2}O_2 \xrightarrow{k_{f1}} CO \tag{7.21}$$

$$C_s + CO_2 \xrightarrow{k_{f2}} CO \tag{7.22}$$

where C_s is in solid phase carbon. The oxidizers are not limited to O_2 and CO_2; other species such as OH, O, and H_2O can also be effective oxidizers.

The oxidation takes place at the surface of the solid char and the corresponding rate of reaction is governed by the diffusion of oxidizers to the surface of the char.

The apparent rate of char oxidation can be estimated using the equation given by Flagan and Seinfeld [13]

$$r = A\exp\left(-\frac{E}{RT}\right)\left(P_{O_2}^n\right) \qquad \left(\mathrm{kg/m^2 \cdot s}\right) \tag{7.23}$$

where $P_{O_2}^n$ is the partial pressure of the oxidier, with a unit of atm. A, E/R, and n are constants for specific solid fuels and they can be determined experimentally.

The formation of carbon monoxide and hydrogen carbon is driven by local fuel rich combustion in the flame and imperfect mixing between fuel and oxygen.

The level of CO in the exhaust or flue gas depends on the design of the combustion system. Oxidation of CO to CO_2 takes place in the luminous zone by the following mechanisms [26].

$$\begin{gathered} CO + OH \rightarrow CO_2 + H \\ k_{f1} = 4.4T^{1.5}\exp(372/T) \qquad \mathrm{m^3/mol \cdot s} \end{gathered} \tag{7.24}$$

$$\begin{gathered} H + CO_2; \rightarrow CO + O + H \\ k_{f2} \cong 0 \end{gathered} \tag{7.25}$$

$$\begin{gathered} CO + O_2 \rightarrow CO_2 + O \\ k_{f3} = 2.5 \times 10^6\exp(-24{,}060/T) \qquad \mathrm{m^3/mol \cdot s} \end{gathered} \tag{7.26}$$

$$\begin{gathered} CO + O + M \rightarrow CO_2 + M \\ k_{f4} = 53\exp(2{,}285/T) \qquad \mathrm{m^6/mol \cdot s} \end{gathered} \tag{7.27}$$

$$\begin{gathered} CO + HO_2 \rightarrow CO_2 + OH \\ k_{f5} = 1.5 \times 10^8\exp(-11{,}900/T) \qquad \mathrm{m^3/mol \cdot s.} \end{gathered} \tag{7.28}$$

The rates of formation of O, OH, and H are usually assumed to be at equilibrium and they can be estimated from the following reactions

$$\frac{1}{2}O_2 \leftrightarrow O \qquad K_{P,O} = 3{,}030\exp(-30{,}790/T) \quad \text{atm}^{-\frac{1}{2}} \tag{7.29}$$

$$\frac{1}{2}H_2O \leftrightarrow \frac{1}{4}O_2 + H \qquad K_{P,H} = 44{,}100\exp(-42{,}500/T) \quad \text{atm}^{-3/4} \tag{7.30}$$

$$\frac{1}{2}H_2O + \frac{1}{4}O_2 \leftrightarrow OH \qquad K_{P,OH} = 166\exp(-19{,}680/T) \quad \text{atm}^{1/4}. \tag{7.31}$$

The overall reaction for the oxidation of CO is

$$CO + \frac{1}{2}O_2 \leftrightarrow CO_2 \tag{7.32}$$

It is very sensitive to temperature. The chemical equilibrium constants at different temperatures can be found in Table 3.2 above.

Dryer [10] gave an empirical equations for the consumption rate of CO and the rate of formation of CO_2 as follows

$$-\frac{d[CO]}{dt} = 10^{14.6\pm0.25}\exp\left(-\frac{40{,}000 \pm 1250}{RT}\right)[CO][H_2O]^{\frac{1}{2}}[O_2]^{\frac{1}{4}} \left(\text{mol}/\text{cm}^3 \cdot \text{s}\right) \tag{7.33}$$

$$-\frac{d[CO_2]}{dt} = 10^{14.75\pm0.4}\exp\left(-\frac{43{,}000 \pm 2{,}200}{RT}\right)[CO][H_2O]^{\frac{1}{2}}[O_2]^{\frac{1}{4}} \left(\text{mol}/\text{cm}^3 \cdot \text{s}\right) \tag{7.34}$$

7.6 Formation of SO_2 and SO_3

Nearly all fossil fuels contain sulfur atoms. Some of the sulfur in fuels is eventually oxidized to SO_2 and SO_3. Typical values for the sulphur content of various fuels are given in Table 7.4 [51]. Sulphur in coal is present in both organic and inorganic forms, the latter being pyretic sulphur (FeS_2) and sulphates (Na_2SO_4, $CaSO_4$, $FeSO_4$). Organic sulphur is present in the form of sulphides, mercaptanes, bisulphides, thiophenes, thiopyrones, etc. These organic compounds are also found in crude oils and gases.

Table 7.4 Typical values for sulphur content of fuels (wt%, dry)

Fuel		Sulphur content (wt%, dry)
Fossil fuels	Coal	0.2–5
	Oil	1–4
	Natural gas	0–10
	Light fuel oil	<0.5
	Heavy fuel oil	<5
	Peat	<1
	Petroleum coke	~5
Biomass	Wood	<0.1
	Straw	~0.2
	Bark	<2

The more sulfur in the fuel, the higher level of SO_2 emission. SO_2 is mainly formed when the sulfur elements are oxidized by O_2,

$$S + O_2 \rightarrow SO_2 \tag{7.35}$$

and SO_2 can be oxidized to SO_3.

Their concentrations at equilibrium can be determined by the overall reaction, using the knowledge we learned in Chap. 3.

$$\begin{aligned} &SO_2 + {}^1\!/_2 O_2 \leftrightarrow SO_3 \\ &K_{P,SO_3} = 1.53 \times 10^{-5} \exp\left(\tfrac{11{,}760}{T}\right) \qquad \text{atm}^{-\frac{1}{2}} \end{aligned} \tag{7.36}$$

The van't Hoff equation (7.36) of the chemical equilibrium constant indicates that the concentration of SO_3 increases with the decreasing combustion temperature. The kinetics of SO_2 oxidation without catalytic effect can be described as follows [51].

$$SO_2 + O + M \rightarrow SO_3 + M \quad k_{f1} = 8.0 \times 10^4 \exp(-1{,}400/T)\ \text{m}^6/\text{mol} \cdot \text{s} \tag{7.37}$$

$$SO_3 + O + M \rightarrow SO_2 + O_2 + M \quad k_{f2} = 7.04 \times 10^4 \exp(785/T)\ \text{m}^6/\text{mol} \cdot \text{s} \tag{7.38}$$

$$SO_3 + H \rightarrow SO_2 + OH \quad k_{f3} = 1.5 \times 10^7\ \text{m}^3/\text{mol} \cdot \text{s} \tag{7.39}$$

Assuming constant-temperature and fuel-lean combustion, the net rate of SO_3 formation is thus described by Eq. (7.40)

$$r_{SO_3} = \frac{d[SO_3]}{dt} = k_{f1}[SO_2][O][M] - k_{f2}[SO_3][O][M] - k_{f3}[SO_3][H] \tag{7.40}$$

Sulfur mass conservation gives $[SO_2] + [SO_3] = [S] = \text{constant}$, or $[SO_2] = ([S] - [SO_3])$ and Eq. (7.40) becomes

$$r_{SO_3} = k_{f1}([S] - [SO_3])[O][M] - k_{f2}[SO_3][O][M] - k_{f3}[SO_3][H] \tag{7.41}$$

When the SO_3 concentration reaches steady state, corresponding to $r_{SO_3} = 0$, the equilibrium SO_3 concentration is described in terms of [O] and [H] as

$$[SO_3]_s = \frac{k_{f1}[O][M][S]}{(k_{f1} + k_{f2})[O][M] + k_{f3}[H]} \tag{7.42}$$

This equation can be used to estimate the steady-state SO_3 concentration as a fraction of the total SO_x concentration $[S] = [SO_2] + [SO_3]$. Mostly [O] and [H] are assumed constant.

The formation of sulphuric pollutants during solid fuel combustion can also be described by the following step reactions [51].

Fuel sulfur is first heated and devolatilized through,

$$\text{Fuel} - \text{S(s)} \rightarrow H_2S + COS + \cdots + \text{Char} - \text{S(s)} \tag{7.43}$$

Both solid and gases (vapors) are produced through this reaction. The solid phase char sulfur can be oxidized through the following reactions, where H_2S, SO_2 and COS are produced.

$$\text{Char} - \text{S} + O_2 \rightarrow SO_2 \tag{7.44}$$

$$\text{Char} - \text{S} + CO_2 \rightarrow COS \tag{7.45}$$

$$\text{Char} - \text{S} + H_2O \rightarrow H_2S. \tag{7.46}$$

The gas phases produced during the above three reactions can further react through

$$H_2S + 1^1/_2O_2 \rightarrow SO_2 + H_2O \tag{7.47}$$

$$H_2S + CO_2 \rightarrow COS + H_2O \tag{7.48}$$

$$H_2S + CO \rightarrow H_2 + COS \tag{7.49}$$

$$H_2S + COS \rightarrow CS_2 + H_2O \tag{7.50}$$

$$CS_2 \rightarrow C + 2/x\,S_x. \tag{7.51}$$

In the products, the concentrations of SO_2 and SO_3 at equilibrium can still be determined by the overall reaction in Eq. (7.36)

$$SO_2 + 1/2O_2 \leftrightarrow SO_3 \tag{7.52}$$

For coal combustion, sulfur in fuels is eventually oxidized to SO_2 and/or SO_3, with a small amount being bound to ashes. For combustion of liquid fuels in engine, SO_2 concentration in the engine exhaust depends on the type of fuel burned. Marine engine exhaust usually has the highest SO_2 emission, and it can be in a level that is comparable with coal fired power plants, (about 1 %) because marine diesel fuels are of very low quality and high sulfur content.

The chemical equilibrium constant in Eq. (7.36) indicates that the concentration of SO_3 increases with the decreasing combustion temperature. When the temperature is below 900 K, SO_3 would have been the dominant SO_x air pollutant at equilibrium. However, in a typical flue gas or engine exhaust, SO_2 is still dominating over SO_3. One of the reasons is that the conversion from SO_2 to SO_3 is too slow to reach an equilibrium state. In a typical engineering practice, about 3 % of SO_2 is converted into SO_3. Typical SO_2 concentration in a coal fired power plant flue gas stream is in the order of 1,000 ppm (0.1 %). It shall be much lower in modern gasoline or natural gas fired stationary combustion facilities because sulfur has been removed from the fuels.

The oxidation of SO_2 to SO_3 is usually slow unless the combustion temperature is above 1,100 °C or there are catalysts present to expedite the reaction. For example, sulphur in the liquid fuels supplied to automobiles is oxidized to SO_2 in the engine. But in the exhaust SO_3 is present due to the presence of various catalytic metals in the fuel, engine housing, and/or the filtration systems. For stationary combustion sources like a coal-fired power plant, there are also various metals in the fuel, and some of them may serve as catalysts for the oxidation of SO_2.

7.7 NO_x

Nitrogen oxides (NO_x) represent the following seven oxides of nitrogen [45].

- nitric oxide (NO)
- nitrogen dioxide (NO_2)
- nitrous oxide (N_2O)
- dinitrogen dioxide (N_2O_2)
- dinitrogen trioxide (N_2O_3)
- dinitrogen tetroxide (N_2O_4)
- dinitrogen pentoxide (N_2O_5)

However, NO_x are often referred only to NO and NO_2 by the environmental protection agencies in most jurisdictions. It is because these two gases are the major contributors to air pollution. Therefore, only NO and NO_2 are introduced in the following section.

7.7.1 Nitric Oxide

7.7.1.1 Thermal NO

For the analysis above using simple chemical stoichiometry (Chap. 3), it was assumed that nitrogen (N_2) is inert and does not react with oxygen. This is no longer true when the reaction temperature is high enough. As a result, NO is produced by the oxidation of N_2 in the air through the following chemical reaction,

$$\begin{gathered}\frac{1}{2}N_2 + \frac{1}{2}O_2 \leftrightarrow NO \\ K_{P,NO} = 4.71\exp\left(-\frac{10{,}900}{T}\right)\end{gathered} \tag{7.53}$$

As indicated by the formula for equilibrium constant ($K_{P,NO}$), oxidation of nitrogen proceeds slowly at low temperatures, but very fast at high temperatures. The formation of NO from molecular nitrogen was first proposed by Zeldovich [50], and it is thus referred to as the Zeldovich mechanism. NO formed by this mechanism is also called thermal NO.

Thermal NO formation was first introduced in the 1940s. The formation of thermal NO is very sensitive to the combustion temperature, and its formation is negligible when temperature is 1,000 °C or lower. On the other hand, the rate of NO formation is significant and increases exponentially when the temperature is over 1,400 °C [20]. The reactions in Table 7.5 can be used to describe the step reactions of thermal NO formation.

First of all, the concentration of oxygen atoms required for the initiation of reaction is strongly dependent on temperature because more oxygen atoms are available to the reaction at higher temperature. Secondly, this reaction produces nitrogen atoms, which is the bottleneck that limits the rate of NO formation, which is also sensitive to temperature.

Table 7.5 Thermal NO step reactions and rate constants

Reaction	Rate constant $\left(m^3/mol \cdot s\right)$	Equation
$N_2 + O \underset{k_{b1}}{\overset{k_{f1}}{\leftrightarrow}} NO + N$	$k_{f1} = 1.8 \times 10^8 \exp\left(-\frac{38{,}370}{T}\right)$	(7.54)
	$k_{b1} = 3.8 \times 10^7 \exp\left(-\frac{425}{T}\right)$	
$N + O_2 \underset{k_{b2}}{\overset{k_{f2}}{\leftrightarrow}} NO + O$	$k_{f2} = 1.8 \times 10^4 T \times \exp\left(-\frac{4{,}680}{T}\right)$	(7.55)
	$k_{b2} = 3.8 \times 10^3 T \times \exp\left(-\frac{-20{,}820}{T}\right)$	
$N + OH \underset{k_{b3}}{\overset{k_{f3}}{\leftrightarrow}} NO + H$	$k_{f3} = 7.1 \times 10^7 \times \exp\left(-\frac{450}{T}\right)$	(7.56)
	$k_{b3} = 1.7 \times 10^8 \times \exp\left(-\frac{24{,}560}{T}\right)$	

The net rate of NO formation under a constant pressure and temperature condition can be calculated by considering all three step reactions in Table 7.5.

$$\begin{aligned} r_{\mathrm{NO}} = \frac{\mathrm{d[NO]}}{\mathrm{d}t} = &\{k_{1\mathrm{f}}[\mathrm{N_2}][\mathrm{O}] - k_{1\mathrm{b}}[\mathrm{NO}][\mathrm{N}]\} \\ &+ \{k_{2\mathrm{f}}[\mathrm{O_2}][\mathrm{N}] - k_{2\mathrm{b}}[\mathrm{NO}][\mathrm{O}]\} \\ &+ \{k_{3\mathrm{f}}[\mathrm{N}][\mathrm{OH}] - k_{3\mathrm{b}}[\mathrm{NO}][\mathrm{H}]\}. \end{aligned} \tag{7.57}$$

When all the reactions in Table 7.5 reach equilibrium state, the NO formation rate attributed to each of three step reactions can be described as, respectively,

$$\begin{aligned} r_1 &= k_{1\mathrm{f}}[\mathrm{N_2}]_{\mathrm{e}}[\mathrm{O}]_{\mathrm{e}} = k_{1\mathrm{b}}[\mathrm{NO}]_{\mathrm{e}}[\mathrm{N}]_{\mathrm{e}} \\ r_2 &= k_{2\mathrm{f}}[\mathrm{O_2}]_{\mathrm{e}}[\mathrm{N}]_{\mathrm{e}} = k_{2\mathrm{b}}[NO]_{\mathrm{e}}[O]_{\mathrm{e}} \\ r_3 &= k_{3\mathrm{f}}[N]_{\mathrm{e}}[\mathrm{OH}]_{\mathrm{e}} = k_{3\mathrm{b}}[\mathrm{NO}]_{\mathrm{e}}[\mathrm{H}]_{\mathrm{e}} \end{aligned} \tag{7.58}$$

where the subscript e stands for equilibrium. For easy analysis, we also define two dimensionless concentrations as follows.

$$a = \frac{[\mathrm{NO}]}{[\mathrm{NO}]_{\mathrm{e}}}; \quad b = \frac{[\mathrm{N}]}{[\mathrm{N}]_{\mathrm{e}}} \tag{7.59}$$

Then the rate of NO formation before reaching equilibrium state Eq. (7.57) can be rewritten as

$$r_{\mathrm{NO}} = r_1(1 - ab) + r_2(b - a) + r_3(b - a) \tag{7.60}$$

The concentration of N atoms is needed in order to solve this equation. By similar approach, we can get the rate of N atom formation

$$r_{\mathrm{N}} = r_1(1 - ab) + r_2(a - b) + r_3(a - b) \tag{7.61}$$

By the pseudo-steady-state approximation, we can set the left hand side of Eq. (7.61), $r_N = 0$, and it leads to

$$b = \frac{r_1 + r_2 a + r_3 a}{r_1 a + r_2 + r_3} \tag{7.62}$$

Substitute Eq. (7.62) into Eq. (7.60), and we have the corresponding rate of NO formation as

$$r_{\mathrm{NO}} = \frac{2r_1(r_2 + r_3)(1 - a^2)}{ar_1 + r_2 + r_3} \tag{7.63}$$

This equation can also be expressed in terms of dimensionless NO concentration, $a = [NO]/[NO]_e$

$$\frac{da}{dt} = \frac{1}{[NO]_e}\left\{\frac{2r_1(r_2 + r_3)(1 - a^2)}{ar_1 + r_2 + r_3}\right\} \tag{7.64}$$

Integration of this equation with an initial condition of $a = 0$ at $t = 0$ leads to the description of the NO concentration at any time.

$$\left(1 - \frac{r_1}{r_2 + r_3}\right)\ln(1 + a) - \left(1 + \frac{r_1}{r_2 + r_3}\right)\ln(1 - a) = \left(\frac{4r_1}{[NO]_e}\right)t \tag{7.65}$$

For easier expression, we can define the characteristic time for thermal NOx formation as,

$$\tau_{NO} = \frac{[NO]_e}{4r_1} \tag{7.66}$$

and the reaction rate ratio,

$$\rho_r = \frac{r_1}{r_2 + r_3} \tag{7.67}$$

By considering τ_{NO} and ρ_r, Eq. (7.65) becomes

$$(1 - \rho_r)\ln(1 + a) - (1 + \rho_r)\ln(1 - a) = t/\tau_{NO} \tag{7.68}$$

In a typical combustion process, the residence time is shorter than the characteristic time. As a result, NO does not reach its equilibrium concentration. Therefore, it is better for the actual NO concentration in the flame to be determined using this equation.

7.7.1.2 Prompt NO

Fenimore [12] found that some of the NO formed during combustion could not be explained by the aforementioned Zeldovich mechanisms. When equivalence ratio is greater than 1, the nitrogen in the air reacts to form hydrogen cyanide (HCN) through the following chemical reaction,

$$N_2 + CH \leftrightarrow HCN + N \tag{7.69}$$

Since there are oxygen-containing compounds in the combustion system, HCN produced in the above reaction and the nitrogen atom reacts further to produce NO through several chain reactions.

$$O_2 + N \leftrightarrow NO + O \tag{7.70}$$

$$HCN + OH \leftrightarrow CN + H_2O \tag{7.71}$$

$$CN + O_2 \leftrightarrow NO + CO \tag{7.72}$$

Prompt NO is formed only in a combustion zone of the flame where the combustion is incomplete and the hydrocarbon radicals are present [3]. These reactions take place very fast, thus it is known as prompt NO. The formation of prompt NO does not depend on temperature as significantly as the thermal NO. The prompt NO is formed mainly under lower temperature conditions during a short residence time [24].

7.7.1.3 NO Through Intermediate Component N_2O

The third mechanism is through N_2O [20, 32], also known as laughing gas, produced by the reaction between oxygen atoms and N_2:

$$O + N_2 + M \leftrightarrow N_2O + M \tag{7.73}$$

$$N_2O + O \leftrightarrow 2NO \tag{7.74}$$

where M can be any coexisting gas compound. Depending on the condition, N_2O could react again either forward to NO or backward to N_2, and the later often dominates. In general, the formation of NO increases with the air to fuel ratio and temperature.

N_2O is one of the greenhouse gases (GHGs). It can also be formed through other mechanisms, including oxidation of HCN and oxidation of char residue. Part of the volatile cyanide compounds of the fuel nitrogen, such as HCN, is oxidized homogeneously to N_2O through the following reactions:

$$HCN + O \leftrightarrow NCO + H \tag{7.75}$$

Table 7.6 Typical values for the nitrogen content of fuels (dry wt%)

Fuel	N content, wt%, dry
Coal	0.5–3
Oil	<1
Natural gas	0.5–20
Light fuel oil	~0.2
Heavy fuel oil	~0.5
Peat	1–2
Petroleum coke	~3
Wood	0.1–0.5
Straw	0.5–1
Bark	~0.5

$$NCO + NO \leftrightarrow N_2O + CO \tag{7.76}$$

The reaction is also very sensitive to temperature and it slows down significantly when the temperature rises. The reaction stops when the temperature is above 950 °C, and the NCO radicals are converted to NO.

7.7.1.4 Fuel NO

Most fuels contain nitrogen element, the NO originated from this part of nitrogen is referred to as fuel NO [19, 33, 37, 44]. The amount of nitrogen in fuel varies with the fuel type. As summarized in Table 7.6 [51], typical coal and oil contain chemically bound organic nitrogen, which is different from that found in natural gas. Depending on the refinery process, some natural gases contain virtually no nitrogen but others have quite a lot of nitrogen in form of N_2. Unlike fossil fuels, biomass is characterized with high nitrogen.

Although the amount of nitrogen in fuel is relatively small, the fuel nitrogen is much more reactive compared to the nitrogen present in the combustion air. Consequently, the formation of fuel NO from a nitrogen-rich fuel is higher than that from a nitrogen-lean fuel. Sometimes, as much as 80 % of the NO in the flue gas of a coal-firing furnace is produced from fuel nitrogen [33]. The fuel NO is sensitive to stoichiometry rather than the temperature because it forms readily at quite low temperatures [7].

For a simple comparison purpose, Fig. 7.4 shows the relative importance of thermal NO, prompt NO and fuel NO formation at different temperatures. Overall NO emissions increase with temperature, mainly due to the increase of thermal NO. Typical NO concentrations in the flue gases produced by the combustion of coal, oil, and natural gas before flue gas cleaning are in the order of hundreds of ppmv. The temperature in a typical industrial furnace is about 1,400–1,500 °C where the magnitude of the NO equilibrium concentration is about 1,000 ppmv. However, the

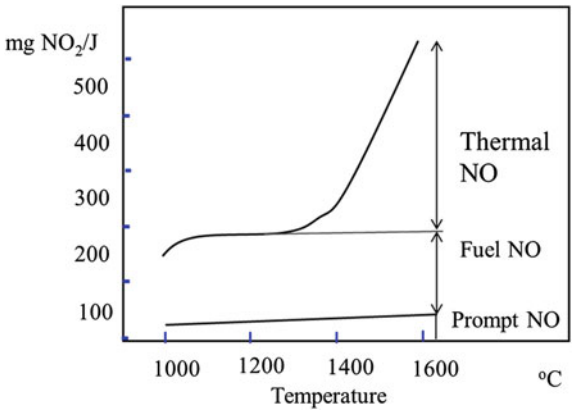

Fig. 7.4 Influence of temperature on *thermal* NO_x, *prompt* NO_x and *fuel* NO_x formation

NO equilibrium concentration drops sharply as the temperature goes down, and becomes negligible below 600 °C.

7.7.1.5 NO*x* Formation in Char Combustion

Char is formed during combustion of solid fuels, especially coal. This char residue forms N_2O under appropriate conditions. The N_2O formed from char nitrogen varies, depending on fuel property and devolatilization conditions. However, the formation mechanism of N_2O from char nitrogen is not yet fully clarified and different mechanisms have been proposed in literature.

Much of the NO formation in coal combustion is by char–nitrogen interaction [48]. Nitrogen atoms can be adsorbed by char, which is porous anyway. The char–nitrogen is oxidized to produce NO, and it can be described with a simplified reaction formula as

$$(\mathrm{N}+\mathrm{C})+\frac{1}{2}\mathrm{O_2}\rightarrow \mathrm{NO}+\mathrm{C_s} \tag{7.77}$$

where (N + C) represents nitrogen atom bounded with carbon by chemisorption on char. NO reduction may take place by the following two reactions

$$2\mathrm{NO}+2\mathrm{CO}\rightarrow \mathrm{N_2}+2\mathrm{CO_2} \tag{7.78}$$

$$\begin{aligned} &2\mathrm{NO}+\mathrm{C_s}\xrightarrow{k_{f6}}(\mathrm{O}+\mathrm{C})+\frac{1}{2}\mathrm{N_2}\\ &k_{f6}=0.21\exp\left(-1.31\times10^4/T\right)\qquad \mathrm{kmol}/\left(\mathrm{m^2\cdot s\cdot atm}\right)\end{aligned} \tag{7.79}$$

where (O + C) is the oxygen bounded with char carbon by chemisorption, and it reacts with CO to produce CO_2

$$\begin{aligned} &\mathrm{CO}+(\mathrm{O}+\mathrm{C})\xrightarrow{k_{f7}}\mathrm{CO_2}+\mathrm{C_s}\\ &k_{f7}=7.4\times10^{-4}\exp\left(-9.56\times10^3/T\right)\qquad \mathrm{kmol}/\left(\mathrm{m^2\cdot s\cdot atm}\right)\end{aligned} \tag{7.80}$$

With the increasing temperature, the oxygen adsorbed onto the surface of carbon may also produce CO directly,

$$\begin{aligned} &(\mathrm{O}+\mathrm{C})\xrightarrow{k_{f8}}\mathrm{CO}\\ &k_{f8}=1.5\times10^{-2}\exp\left(-2.01\times10^4/T\right)\qquad \mathrm{kmol}/\left(\mathrm{m^2\cdot s\cdot atm}\right)\end{aligned} \tag{7.81}$$

Then, the overall rate of NO reduction can be determined as follows [48].

$$-r_{\mathrm{NO}}=\frac{k_{f6}P_{\mathrm{NO}}\left(k_{f7}P_{\mathrm{CO}}+k_{f8}\right)}{k_{f6}P_{\mathrm{NO}}+k_{f7}P_{\mathrm{CO}}+k_{f8}} \tag{7.82}$$

The overall rate of NO formation from char-bound nitrogen is also described by Williams et al. [48]

$$r_{NO} = -\frac{[N]_{char}}{[C]_{char}} r_{char} \tag{7.83}$$

where the reaction rate of char is

$$r_{char} = 254 \exp\left(-2.16 \times 10^{-2}/T\right) P_0^n \tag{7.84}$$

The analysis above is also applicable to biomass combustion with the following differences. First of all, most (80 % or more) of the biomass is volatile and there is little char left. The combustion of char fraction is minor compared to volatile combustion.

7.7.2 Nitrogen Dioxide

The oxidation of NO leads to the formation of NO_2 through the overall reaction

$$\begin{aligned} &NO + \frac{1}{2}O_2 \leftrightarrow NO_2 \\ &K_{P,NO_2} = 2.5 \times 10^{-4} \exp\left(\frac{6923}{T}\right) \qquad \text{atm}^{-1/2} \end{aligned} \tag{7.85}$$

The corresponding step reactions are

$$\begin{aligned} &NO + NO + O_2 \leftrightarrow NO_2 + NO_2 \\ &k_f = 1.2 \times 10^{-3} \exp(530/T) \qquad \text{m}^6/\text{mol} \cdot \text{s} \end{aligned} \tag{7.86}$$

$$\begin{aligned} &NO + O + M \leftrightarrow NO_2 + M \\ &\left\{ \begin{array}{ll} k_f = 1.5 \times 10^3 \exp(940/T) & \text{m}^6/\text{mol} \cdot \text{s} \\ k_b = 1.1 \times 10^{10} \exp(-33{,}000/T) & \text{m}^3/\text{mol} \cdot \text{s} \end{array} \right\} \end{aligned} \tag{7.87}$$

The conversion of NO to NO_2 can also take place when there are enough hydrogen peroxide radicals (HO_2).

$$\begin{aligned} &NO + HO_2 \leftrightarrow NO_2 + OH \\ &k_f = 2.1 \times 10^6 \exp(240/T) \qquad \text{m}^3/\text{mol} \cdot \text{s} \end{aligned} \tag{7.88}$$

Hydrogen peroxide radical is formed when a hydrogen atom reacts with oxygen in the presence of a third component (M).

$$H + O_2 + M \leftrightarrow HO_2 + M \tag{7.89}$$

This reaction is significant at low temperatures. As a result, considerable HO_2 concentration may be present in the low temperature zones of the flame, and consequently a significant part of the NO present in the cooler zones may react into NO_2 through Eq. (7.88).

In the high temperature zone of the flame, hydrogen and oxygen tends to react directly to form hydroxyl radicals and oxygen atoms:

$$H + O_2 \rightarrow OH + O \tag{7.90}$$

The NO_2 formed at lower temperature decomposes rapidly back to NO when it drifts into the high temperature zone of the flame.

$$NO_2 + H \rightarrow NO + OH \tag{7.91}$$

$$NO_2 + O \leftrightarrow NO + O_2 \tag{7.92}$$

Partially due to this decomposition process, NO_2 remains less than 5 % with 95 % or more NO in a typical flue gas. However, these reactions slow down at low concentrations of O and H. This situation arises when hot and cold streams are mixed rapidly.

7.8 Formation of Particulate Matter

In combustion inorganic minerals in fuel are converted into solid, liquid, and vapors. The solid and liquid contribute directly to the particulate matter formation, while the vapors could condense, solidify, and form secondary particulate matter before and after the emission. The final phase of the ash-forming materials depends on many factors including temperature, pressure, residence time, fuel particle size and size distribution, and the compounds in the combustion system. For solid fuels the ash-forming minerals are mainly converted to oxides of silicon, aluminum, and iron (SiO_2, Al_2O_3 and Fe_2O_3). For liquid and gaseous petroleum fuels, the particulate matter is mainly due to the incomplete combustion and secondary reaction of VOCs and SO_x/NO_x. However, this general knowledge may not apply to alternative and renewable fuels.

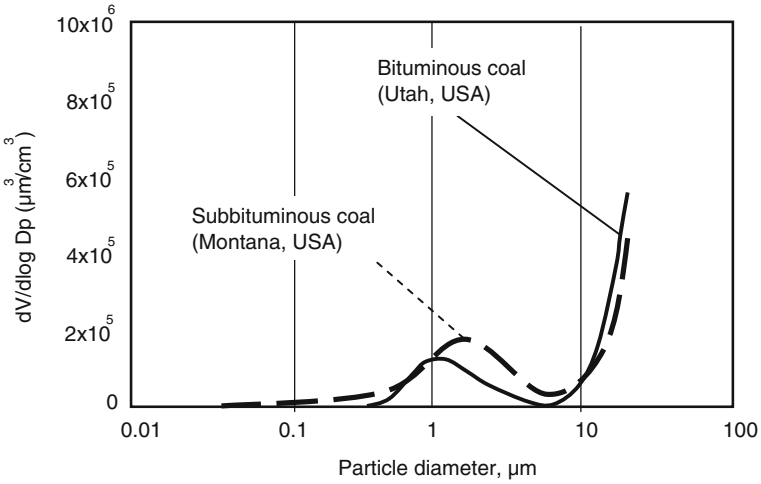

Fig. 7.5 Fly ash particle size distribution (*Data source* Linak et al. [31])

7.8.1 Ash-Forming Elements in Fuels

Fossil fuels contain highly integrated ash-forming matter in form of discrete particles, and bounded combustible compounds. A review of the corresponding particle forming mechanisms can be found in literature [9].

The discrete mineral particles if not removed by fuel cleaning are quickly molten at high temperatures, followed by condensation while traveling in the ducting systems as temperature drops before emitting to the atmosphere. The relative quantities of the bounded minerals increase while hydrocarbon is consumed by oxygen in combustion. Metal oxides can also contribute to the formation of $PM_{2.5}$. The elemental metal vapors are also oxidized and consequently form $PM_{2.5}$ by coagulation. Noncombustible solid compounds in the fuel will form the major part of the fly ash particles, ranging from 10 nm to more than 100 μm.

Most fly ash particles are smaller than 0.1 μm in diameter by number, but larger than 1 μm in diameter by mass. This is similar to the size distribution shown in Fig. 7.5, although the exact size distribution depends on the coal and the design and operation of the boiler. The fly ash size distribution in Fig. 7.5 was measured using bituminous and subbituminous coals in the USA.

The ash formation is also dependent on the combustion device. For example, the fate of ash-forming materials in fluidized bed combustion (FBC) is much different from that of pulverized fuel combustion. In FBC, mechanical abrasion and attrition play a more important role than the mechanism introduced above, and the ash-forming materials remain in the fluidized bed. In circulating fluidized bed combustion, more fly ash is formed due to the higher velocities and smaller fuel particle size.

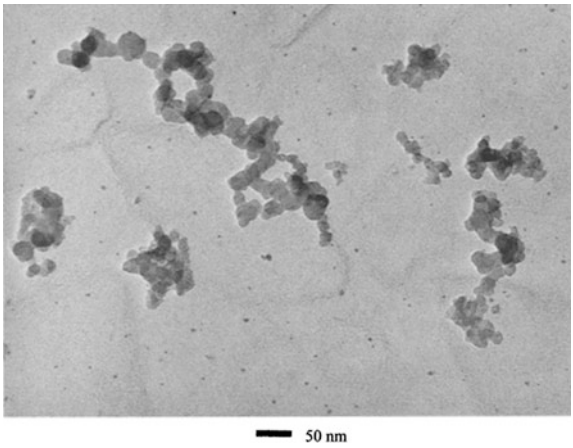

Fig. 7.6 TEM image of soot particles from a diesel engine (used with permission from ACS)

The composition of the ash particles depends strongly on the fuel, although SiO_2, Al_2O_3, Fe_2O_3 and CaO are usually the primary components. Ash from oils contains vanadium (V) and nickel (Ni), plus magnesium (Mg). These metals are added to the fuel as a corrosion inhibitor.

7.8.2 Soot Particles

Carbonaceous particles (10–80 nm) in the combustion system can agglomerate and form larger particles (could be larger than 10 μm) [4, 5, 18]. These clusters are called soot. A soot "particle" could have a family of thousands of carbonaceous particles in it. A transmission electron microscope (TEM) image of diesel engine soot is shown in Fig. 7.6 [41].

Chemically, soot particles are mainly composed of carbon, sulphur, and nitrogen compounds and trace elements. Hydrocarbons can also be adsorbed into soot. These particles could be as small as less than 10 nm in diameter.

There are mainly two mechanisms for the soot formation, depending on the type of fuel [25, 28]. Aliphatics in gaseous or light liquid fuels can be converted to acetylene (C_2H_2) at high temperature, followed by a "polymerization" of C_2H_2 to form soot. This mechanism is also possible for combustion at high temperatures, up to 1,600 °C.

For heavy oil and coal that contain more aromatics than aliphatics, soot is formed by condensation and other processes that have aromatics as the starting point [4, 11, 15, 22, 28, 38, 52]. The overall reaction of soot formation during sub-stoichiometric stages of combustion can be written as

$$C_nH_m + yO_2 \rightarrow 2yCO + {}^1\!/\!_2 mH_2 + (n - 2y)C(s) \quad \text{with } n > 2y \qquad (7.93)$$

Readers are referred to specialized books for more knowledge.

7.9 Fate of Trace Elements

Chemical elements present in a natural material can be classified as trace elements, minor elements, and the major elements, corresponding to concentrations of <0.1, 0.1–1, and >1 wt%, respectively.

Although these trace elements present in the natural ecosystem, quite amount is relocated after fossil fuel combustion. Within the European Community the 13 elements of highest concern are As, Cd, Co, Cr, Cu, Hg, Mn, Ni, Pb, Sb, Sn, Tl, and V. Eleven of 189 hazardous air pollutants (HAPs) in the USA are metals: As, Be, Cd, Co, Cr, Hg, Mn, Ni, Pb, Sb, Se.

7.9.1 Trace Elements in Fuels

Fossil fuels like coal and heavy oil contain trace elements in the forms of organic salts and inorganic minerals, for example, pyrites, and other sulphides, (alumino-) silicates and carbonates [47]. In typical coal the concentrations of Pb, B, Cr, Ni, and V are high. Ni and V are also found in oils.

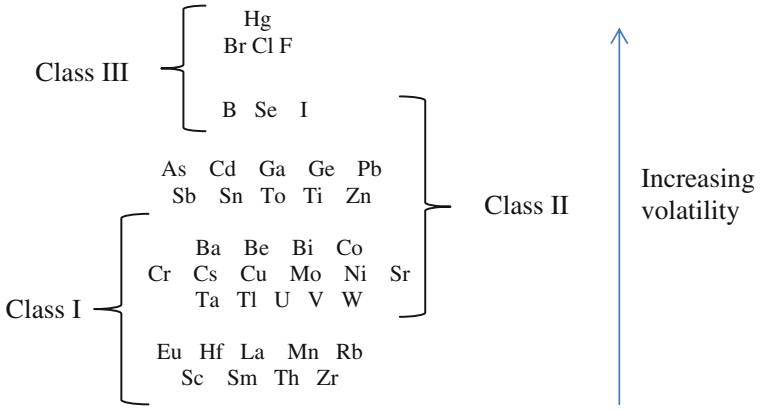

Fig. 7.7 Classification of trace elements

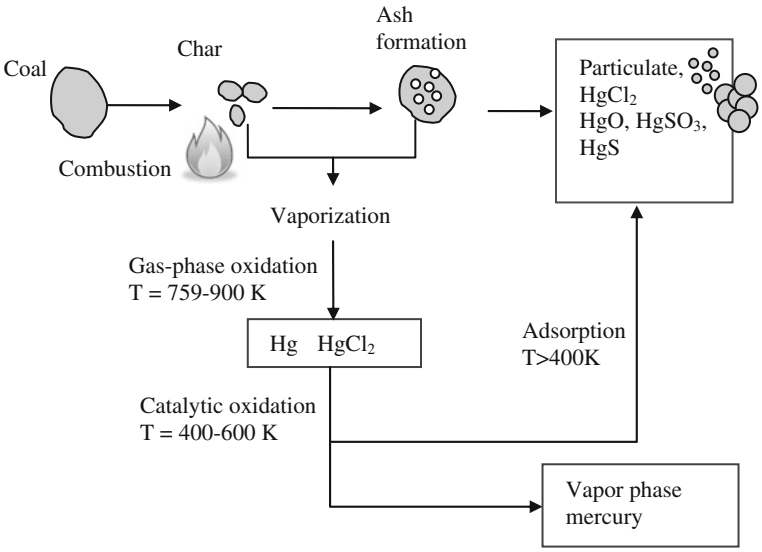

Fig. 7.8 Most probable mercury-species transformations in- and post- coal combustion

7.9.2 Trace Elements in Flue Gases

The fate of trace elements in combustion is influenced by many factors. Temperature is the main factor that determines whether a certain trace element will be volatilized. The other important factor that determines volatility is the air to fuel ratio. Many trace elements are more volatile under fuel rich condition than fuel lean condition. A third important factor is the presence of chlorine. Chlorine often reacts with a significant fraction of the trace elements to form chlorides, which are more volatile than the elemental or oxide form of the trace elements. The fourth factor of importance is total system pressure. Particle size has negligible effect on the vaporization of trace elements [40].

Based on the fate, trace elements may be classified into three categories as shown in Fig. 7.7.

- Class I—these elements do not volatilize during combustion, and they end up being captured with bottom ashes and fly ashes. The injection of sorbent (calcium) for SO_2 capture will expedite this process.
- Class II—these elements are vaporized during combustion and eventually captured by the particulates by condensation and nucleation mechanisms as the temperature drops along the duct of flue gases.
- Class III—these elements are vaporized but cannot be captured by the particulates (fly ash) in the flue gas. They enter the atmosphere, and become hazardous air emissions.

There are some overlaps between these three classes of trace elements. For example, B, Se, and I can be classified into Class II or Class III [39]. Combined with information on toxicity and harmful effects on process equipment, this classification gives first indication on which trace elements will need special attention.

7.9.3 Mercury

Mercury (Hg), a Class III trace element, is very problematic due to its toxicity and volatility (boiling point 357 °C). In combustion more than 90 % of the incoming Hg penetrates through the flue gas cleaning system, and is discharged into the atmosphere as vapor. Due to its high volatility, Hg is released from fossil fuels at about 150 °C, mainly as elemental Hg, $HgCl_2$, Hg_2Cl_2 and HgS. The release of Hg from the fuel will be complete at 500–600 °C [17, 35]. Under oxidizing conditions, in the presence of HCl and Cl_2, elemental Hg is oxidized to $HgCl_2$ at 300–400 °C (Fig. 7.8).

$$Hg + 4HCl + O_2 \leftrightarrow 2\ HgCl_2 + 2H_2O \tag{7.94}$$

$$Hg + Cl_2 \leftrightarrow HgCl_2 \tag{7.95}$$

Elemental mercury may react with NO_2 through the following reactions [6]:

$$NO_2 + Hg \leftrightarrow HgO + NO \tag{7.96}$$

The product of HgO continues to react with HCl as follows.

$$HgO + 2HCl \leftrightarrow HgCl_2 + H_2O \tag{7.97}$$

As a result, three different mercury species must be considered in the flue gas from coal combustion: gaseous elemental mercury (Hg), gaseous oxidized mercury (e.g., $HgCl_2$, HgS, HgO, $HgSO_4$) and particle-bound mercury (Hg-p). It is estimated that Hg emissions from a coal-fired power plant leaving the furnace, entering the flue gas duct are of the order 5–50 $\mu g/m^3$ at STP.

7.10 Greenhouse Gases

By the end of the twentieth century it was widely accepted that CO_2, CH_4, nitrous oxide (N_2O), and water contribute to the global warming. Water vapor is the most abundant greenhouse gas in the atmosphere, and it contributes to 2/3 of the greenhouse effects. The rest of 1/3 effect caused by other GHGs is referred to as the "enhanced greenhouse effect", or the "anthropogenic greenhouse effect". CO_2 is contributing nearly ¾ of the enhanced greenhouse effect.

The major source for CO_2 emission is the combustion of hydrocarbon fossil fuel. CO_2 concentrations in flue gases from natural gas-fired combined cycle power plants are about 4 % by volume, however it increases to 9–14 % from coal fired boilers. These amounts of CO_2 are currently emitted to the atmosphere without control.

Overall, the fossil-fuel combustion produces a variety of air pollutants in a great quantity. A typical 1,000-MW coal-fired power plant can produce about hundreds of thousand tons per year of particulate matter, sulfur dioxide, as well as comparable quantities of nitrogen oxides, carbon monoxide, volatile compounds, and trace metals. These air emissions have to be reduced as much as possible to protect public health and the environment. They are achieved by pre-, in- and post-combustion control approaches. They are covered in the following chapters.

References and Further Readings

1. ASTM International standard (MNL 11271 M, Proximate Analysis). doi:10.1520/MNL11271M
2. ASTM International Standard (MNL11272M, Ultimate Analysis). doi:10.1520/MNL11272M
3. Blevins LG, Renfro MW, Lyle KH, Laurendeau HM, Gore JP (1999) Experimental study of temperature and CH radical location in partially premixed CH_4/air coflow flames. Combust Flame 118:684–696
4. Bockhorn H (1994) Soot formation in combustion. Springer, Berlin
5. Bockhorn H, Schafer T (1994) Growth of soot particles in premixed flames by surface reactions. In: Bockhorn H (ed) Soot formation in combustion. Springer, Berlin/Heidelberg
6. Brown TD, Smith DN, Hargis RA Jr, O'Dowd WJ (1999) Mercury measurement and its control: what we know, have learned and need to further investigate. J Air Waste Manag Assoc 49(12):1469–1473
7. Buhre B, Elliott L, Sheng CD, Gupta RP, Wall TF (2005) Oxy-fuel combustion technology for coal-fired power generation. Prog Energy Combust Sci 31:283–307
8. Cooper CD, Alley FC (2002) Air Pollution control—a design approach, 3rd edn. Waveland Press, Illinois
9. Damle AS, Ensor DS, Ranade MB (1981) Coal combustion aerosol formation mechanisms: a review. Aerosol Sci Technol 1(1):119–133
10. Dryer FL (1972) High temperature oxidation of carbon monoxide and methane in a turbulent flow reactor. AMS report T-1034. March 1972
11. D'Anna A, D'Alessio A, Minutulo P (1994) Spectroscopic and chemical characterization of soot inception processes in premixed laminar flames at atmospheric pressure. In: Bockhorn H (ed) Soot formation in combustion. Springer, Berlin
12. Fenimore CP (1971) Formation of nitric oxide in premixed hydrocarbon flames. In: 13th symposium (international) on combustion. The Combustion Institute, Pittsburgh, p 373
13. Flagan RC, Seinfeld JH (2012) Fundamentals of air pollution engineering. Prentice Hall, Englewood Cliffs
14. Fletcher TH (1985) Sensitivity of combustion calculations to devolatilization rate. Expressions. In: Presentation at the American Flame Research Committee, 1985 Fall Meeting, October 17–18, Sandia National Laboratories, Livermore, California, USA
15. Frenklach M, Ebert LB (1988) Comment on the proposed role of spheroidal carbon clusters in soot formation. J Phys Chem 92:561
16. GEO (2000) Global Environment Outlook. Available at http://www.grid.unep.ch/geo

17. Galbreath KC, Zygarlicke CJ (1996) Mercury speciation in coal combustion and gasification flue gases. Environ Sci Technol 38(8):2421–2426
18. Gelencser A (2004) Carbonaceous aerosol. Springer, Berlin 350
19. Glarborg P, Miller JA, Kee RJ (1986) Kinetic modeling and sensitivity analysis of nitrogen oxide formation in well stirred reactors. Combust Flame 65:177–202
20. Glarborg P (1993) NO*x* chemistry in pulse combustion. In: Workshop on pulsating combustion and its applications. Lund, Sweden, August 1993
21. Habib MA, Elshafei M, Dajani M (2008) Influence of combustion parameters on NO_x production in an industrial boiler. Comput Fluids 37:12–23
22. Harris SJ, Weiner AM, Ashcraft CC (1986) Soot particle inception kinetics in a premixed ethylene flame. Combust Flame 64:65–81
23. Harvey D (2014) UCDavis ChemWiki. http://chemwiki.ucdavis.edu/Analytical_Chemistry/Analytical_Chemistry_2.0/08_Gravimetric_Methods/8C_Volatilization_Gravimetry. accessed 12 June 2014
24. Hayhurst AN, Vince IM (1980) Nitric oxide formation from N_2 in flames: the importance of 'prompt' NO, progress in energy combust. Science 6:35–51
25. Haynes BS, Wagner H (1981) Soot formation. Prog Energy Combust Sci 7(4):229–273
26. Heinsohn R, Kabel R (1999) Sources and control of air pollution. Prentice Hall, Upper Saddle River
27. Higman C, van Burgt M (2008) Coal gasification 2nd edn. Gulf Professional Publishers, Houston
28. Homann KH (1984) Formation of large molecules, particulates, and ions in premixed hydrocarbon flames; progress and unresolved questions. Proc Combust Inst 20:857–870
29. Hupa M, Backman F, Bostroem S (1989) Nitrogen oxide emissions of biolers in Finland. J Air Pollut Control Assoc 39:1496–1501
30. Kobayashi H, Howard JB, Sarofim AF (1976) Coal devolatilization at high temperatures. In: 16th symposium (Int'l.) on combustion, The Combustion Institute, Symposium (International) on Combustion (16th), held at The Massachusetts Institute of Technology, Cambridge, Massachusets, 15–20 August 1976
31. Linak WP, Miller CA, Seames WS, Wendt JOL, Ishinomori T Endo Y, Miyamae S (2002) On trimodal particle size distributions in fly ash from pulverized-coal combustion. Proc Combust Inst 29:441–447
32. Malte PC, Pratt DT (1975) Measurement of atomic oxygen and nitrogen oxides in jet-stirred combustion. Proc Combust Inst 15:1061–1070
33. Martin GB, Berkau EE (1971) An investigation of the conversion of various fuel nitrogen compounds to nitrogen oxides in oil combustion. In: 70th National American Institute of Chemical Engineers Meeting, Atlantic City, N. J., August, 1971
34. Mauss F, Schafer T, Bockhorn H (1994) Inception and growth of soot particles in dependence on the surrounding gas phase. Combust Flame 99(3–4):697–705
35. Merdes AC, Keener TC, Khang S-J, Jenkins RG (1998) Investigation into the fate of mercury in bituminous coal during mild pyrolysis. Fuel 77(15):1783–1792
36. Migule AH, Kirchstretter TW, Harley RA, Hering SV (1998) On-road emissions of particulate polycyclic aromatic hydrocarbons and black carbon from gasoline and diesel vehicles. Environ Sci Technol 32:450–455
37. Miller JA, Branch MC, McLean WJ, Chandler DW, Smooke MD, Lee RJ (1984) The conversion of HCN to NO and N_2 in H_2–O_2–HCN–Ar flames at low pressure. In: Twentieth symposium (International) on combustion, The Combustion Institute, pp 673–684
38. Pfefferle LD, Bermudez G, Byle J (1994) Benzene and higher hydrocarbon formation during allene pyrolysis. In: Bockhorn H (ed) Soot formation in combustion. Springer, Berlin
39. Ratafia-Brown J (1994) Overview of trace element partitioning in flames and furnaces of utility coal-fired boilers. Fuel Process Technol 39:139–157
40. Senior CL et al (1998) Toxic substances from coal combustion—a comprehensive assessment. In: Proceedings of the 15th annual international Pittsburgh coal conference, Pittsburgh, PA, USA, Sept 1998

41. Shi JP, Mark D, Harrison RM (2000) Characterization of particles from a current technology heavy-duty diesel engine. Environ Sci Technol 34(5):748–755
42. Sirignano W (1983) Fuel droplet vaporization and spray combustion theory. Prog Energy Combust Sci 9:291–322
43. Stickler D, Becker F, Ubhayakar S (1979) Combustion of pulverized coal at high temperature. AIAA Paper No. 79-0298, The American Institute of Aeronautics and Astronautics (AIAA), Reston, VA, USA
44. Turner DW, Andrews RL, Siegmund CW (1971) Influence of combustion modification and fuel nitrogen content on nitrogen oxide emissions from fuel oil combustion. In: Winter American Institute of chemical engineers meeting, San Francisco, December, 1971. AIChE series no 126, vol 68
45. USEPA (1983) Control techniques for nitrogen oxides emissions from stationary sources, 2nd edn. U.S. EPA, Washington D.C. (revised)
46. Ubhayakar SK, Stickler DB, von Rosenberg CW Jr, Gannon RE (1977) Rapid devolatilization of pulverized coal in hot combustion gases. In: Proceedings of the 16th symposium (international) on combustion, The Combustion Institute, Pittsburgh, Pennsylvania, pp 427–436
47. Vassilev SV, Braekman-Danheux C, Laurent P, Thiemann T, Fontana A (1999) Behavior, capture and inertization of some trace elements during combustion of refuse-derived char from municipal solid waste. Fuel 78:1131–1145
48. Williams A, Pourkashanian M, Jones JM (2001) Combustion of pulverised coal and biomass. Prog Energy Combust Sci 27(6):587–610
49. Yuen M, Chen L (1976) On drag of evaporating droplets. Combust Sci Technol 14:147–154
50. Zeldovich YB (1946) The Oxidation of Nitrogen in Combustion Explosions. Acta Physicochimica USSR 21:577
51. Zevenhoven R, Kilpinen P (2002) Flue gas and fuel gas, 2nd edn. Report TKK ENY-4, The nordic energy research programme, Solid Fuel Committees, Norway, pp 3–4
52. Zhang QL, O' Brien SC, Heath JR, Liu Y, Curl RF, Kroto HW, Smalley RE (1986) Reactivity of large carbon clusters: spheroidal carbon shells and their possible relevance to the formation and morphology of soot. J Phys Chem 90(4): 525–528